Bone 187 (2024) 117179

Contents lists available at ScienceDirect

Bone

journal homepage: www.elsevier.com/locate/bone

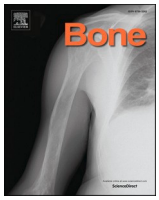

Full Length Article

Evaluation of bone density and microarchitecture in adult patients with X-linked hypophosphatemic rickets: A pilot longitudinal study

Thomas Funck-Brentano [a,b,c,1,*], Arnaud Vanjak [a,b,c,1], Agnes Ostertag [a], Maria Nethander [d], Sylvie Fernandez [b], Corinne Collet [e], Didier Hans [f], Bert van Rietbergen [g], Martine Cohen-Solal [a,b,c]

[a] BIOSCAR UMRS 1132, INSERM, Université Paris Cité, F-75475 Paris, France
[b] Assistance Publique des Hôpitaux de Paris, Lariboisière Hospital, DMU Locomotion, Department of Rheumatology, F-75475 Paris, France
[c] National Reference Center For Rare Bone Diseases, Lariboisière Hospital, APHP.Nord, Filière OSCAR, F-75475 Paris, France
[d] Center for Bone and Arthritis Research, Institute of Medicine, Sahlgrenska Academy, Gothenburg University, Sweden
[e] Imagine Institut, Necker Hospital, Université Paris Cité, F-75475 Paris, France
[f] Center of Bone Diseases, Bone & Joint Department, Lausanne University Hospital, Lausanne, Switzerland
[g] Department of Biomedical Engineering, Eindhoven University of Technology, Eindhoven, the Netherlands

ARTICLE INFO

Keywords:
HRpQCT
DXA
X-linked Hypophosphatemia

ABSTRACT

X-linked Hypophosphatemia (XLH) is the most common type of inherited rickets. Although the clinical features are well characterized, bone structure, mineralization, and biomechanical properties are poorly known. Our aim was to analyze bone properties in the appendicular and axial skeleton of adults with XLH. In this observational case-control study, each affected patient (N = 14; 9 females; age 50 ± 15 years) was matched by sex, age and body mass index to a minimum of two healthy controls (N = 34). Dual-energy X-ray Absorptiometry (DXA) analyses revealed that areal bone mineral density (aBMD) was higher in XLH patients at the lumbar spine (Z score mean difference = +2.47 SD, *P* value = 1.4×10^{-3}). Trabecular Bone Score was also higher at the lumbar spine (*P* value = 1.0×10^{-4}). High Resolution peripheral Quantitative Computed Tomography (HRpQCT) demonstrated that bone cross-sectional area was larger at the distal radius (*P* value = 6×10^{-3}). Total and trabecular volumetric BMD were lower at both sites. Trabecular bone volume fraction was also lower with fewer trabecular numbers at both sites. However, bone strength evaluated by micro-finite element analyzes revealed unaffected bone stiffness and maximum failure load. Evaluation of bone mineralization with aBMD by DXA at the distal radius correlated with vBMD by HRpQCT measurements at both sites. PTH levels were inversely correlated with trabecular vBMD and BV/TV at the tibia. We then followed a subset of nine patients (median follow-up of 4 years) and reassessed HRpQCT. At the tibia, we observed a greater decrease than expected from an age and sex standardized normal population in total and cortical vBMD as well as a trabecularization of the cortical compartment. In conclusion, in adult patients with XLH, bone mineral density is high at the axial skeleton but low at the appendicular skeleton. With time, microarchitectural alterations worsen. We propose that noninvasive evaluation methods of bone mineralization such as DXA including the radius should be part of the management of XLH patients. Larger studies are needed to evaluate the clinical significance of BMD changes in XLH patients under conventional or targeted therapies.

1. Introduction

X-linked Hypophosphatemia (XLH) stands as the most prevalent form of inherited rickets, with an estimated prevalence of approximately 1 in 20,000 individuals [1]. This condition arises from mutations in the *PHEX* gene situated on the X chromosome, leading to FGF23-dependent renal phosphate wasting. Clinical manifestations typically mirror those of osteomalacia or rickets, characterized by dental impairments, bone deformities, and metaphyseal cupping of long bones in children, with pseudofractures and enthesopathy in adults. Traditional treatment

* Corresponding author at: Hôpital Lariboisière, Department of Rheumatology, 2, rue Ambroise Paré, 75010 Paris, France.
E-mail addresses: thomas.funck-brentano@aphp.fr (T. Funck-Brentano), arnaud.vanjak@aphp.fr (A. Vanjak).
[1] Thomas Funck-Brentano and Arnaud Vanjak are the first authors of this article.

https://doi.org/10.1016/j.bone.2024.117179
Received 8 March 2024; Received in revised form 24 June 2024; Accepted 26 June 2024
Available online 1 July 2024

approaches involving calcitriol and phosphate supplementation have shown efficacy in ameliorating radiographic abnormalities and skeletal deformities in children, and to a certain extent, mitigating osteomalacia-related pain in adults [1]. Recently developed therapies targeting FGF23 with neutralizing antibodies have demonstrated effectiveness in correcting serum phosphate levels [2], enhancing linear growth, and alleviating pain in children [3], as well as improving physical function and reducing stiffness in adults [4].

Despite being a key characteristic of the disease, mineralization defects are often inadequately assessed, particularly in adults. The presence of enthesophytes, characterized by ossifications of the longitudinal ligaments, further complicates DXA interpretation, particularly at the spine and hip, where they introduce artifacts leading to an overestimation of bone mineral density (BMD). Due to inconsistent findings across previous studies and contradictory results regarding BMD at axial (high BMD) versus appendicular (normal or low BMD) skeletal sites, the monitoring of patients via DXA scans is not recommended in various national or international management guidelines [5–8]. High-resolution peripheral quantitative computed tomography (HRpQCT) offers precise assessments of bone microarchitecture and density at the distal radius and tibia, areas typically devoid of enthesophytes. Previous investigations employing HRpQCT in XLH subjects, whether children or adults, have yielded conflicting outcomes. Furthermore, longitudinal inquiries tracking alterations in microarchitecture or density among XLH patients are notably scarce.

The primary objective of this study was to utilize noninvasive methods to characterize the areal and volumetric bone mineral densities and microarchitecture in adult patients with XLH, both at baseline and during follow-up. Additionally, our secondary objective aimed to identify which areal DXA measurement sites correlate more closely with bone mineral density and microarchitecture findings obtained through HRpQCT.

2. Methods

2.1. Patients and setting

Adult patients with diagnosed XLH from our National Reference Center for Adults with Rare Bone Diseases were assessed during their routine visits between May 2016 and April 2021. Their diagnosis was based on clinical, radiological and biological features of XLH. Genetic testing confirmed the presence of *PHEX* mutation. Exclusion criteria were age below 18, absence of available HRpQCT scans and a treatment with burosumab. Biochemical assays for serum phosphorus, calcium, creatinine, urine phosphorus and creatinine, serum 25-hydroxyvitamin D (25OHD) and serum parathormone were collected centrally at the inclusion visit according to routine procedures, using our central laboratory's biological standards. Each XLH patient was matched by sex, age, and body mass index, to 2 to 5 healthy controls, who had participated in previous studies of the Rheumatology Department of Lariboisière Hospital [9–12]. Healthy controls were current or former employees of our hospital (physicians, researchers, nurses) or members of their families. To qualify as normal controls, these volunteers were required to have normal aBMD by DXA (Z-score > -1) at each site measured, and no history of non-traumatic fracture. They did not have a systematic X-ray of the spine nor biochemical testing.

All patients and controls gave their written consent to participate to the study and ethical approval was obtained by the local ethical committee [approval number P070121, ethical committee Ile-de-France)].

2.2. DXA evaluation of bone mineral density and Trabecular Bone Score®

DXA scans were conducted on XLH patients and healthy controls to assess bone mineral density (BMD) at various skeletal sites, including the lumbar spine (L1–L4, LS-BMD), total hip (TH-BMD), femoral neck (FN-BMD), distal third radius (Radius 33 %-BMD), and ultra-distal radius (Radius UD-BMD). All measurements were performed using the Lunar Prodigy densitometer (Lunar Corp., Madison, WI, USA), with the same machine and technician ensuring consistency. Age-adjusted values were determined based on a reference population from France, spanning ages 20 to 89 years and sourced from multiple centers (provided by Lunar France). Additionally, Trabecular Bone Score® (TBS) was derived from the lumbar spine DXA images of XLH patients and healthy controls, following established procedures documented in previous publications [13,14].

2.3. High resolution peripheral quantitative CT and finite element analyses

Volumetric BMD (vBMD) and micro-architectural parameters were assessed at the nondominant distal radius and distal tibia by HRpQCT (XtremeCT I, Scanco Medical AG, Brüttisellen, Switzerland) as previously published, and were operated and registered by the same experienced operator. At each site, a stack of 110 parallel CT slices with an isotropic voxel size of 82 μm was obtained, thus delivering a three-dimensional representation of ~9 mm in the axial direction. The most distal CT slice was located 9.5 mm and 22.5 mm proximal to the endplate of the radius and tibia, respectively. Quality control was performed by daily scans of a phantom containing rods of HA (densities of 0 to 800 mg HA/cm^3) embedded in a soft-tissue equivalent resin (QRM, Moehrendorf, Germany) [15].

All scan images were analyzed using the standard patient evaluation protocol provided by the manufacturer as it has been previously described in details [15]. Trabecular and cortical regions of interest were separated automatically by the software, but manually corrected when the contour visually deviated from the apparent endocortical margin, as previously described [16]. Evaluation of both sites resulted in the following parameters: Total bone vBMD (Tt.vBMD, mgHA/cm^3), Cortical bone vBMD (Ct.vBMD, mgHA/cm^3), Trabecular vBMD (Tb.vBMD, mgHA/cm^3), Total bone area (mm^2), Trabecular Area (Tb.Area, mm^2), Cortical bone Area (Ct.Area, mm^2), Cortical bone thickness (Ct.Th, μm), Cortical porosity (Ct.Po, %), Bone volume/Tissue volume (BV/TV, %), Trabecular number (Tb.N, 1/mm^2) Trabecular thickness (Tb.Th, μm), Trabecular Separation (Tb.Sp, μm) and Inhomogeneity of Network (Tb.1/N.SD, μm). Image registration between baseline (T0) and follow-up (T1) scans was done using the 2D technique implemented in the XtremeCT. Levels of overlap during follow-up scans were registered using an area matching technique implemented in the Scanco software, and a cut-off of 75 % was used according to the recent guidelines. [17].

Bone mechanical properties were calculated by micro-finite element analyses. Micro-finite element models were generated directly from the segmented HRpQCT images by converting voxels representing bone tissue into brick elements of the same size. Young's modulus of 10 GPa and Poisson's ratio of 0.3 were assigned to every element. Three different tests were simulated and for each of these test a stiffness was calculated [18]: axial compression (Scomp, kN/mm), bending around the transverse axis (Sbend.Trans, kN mm/rad), bending around the sagittal axis (Sbend, Sag, kN mm/rad), and torsion around the longitudinal axis (Stors, kN mm/rad). Furthermore, the estimated failure load based on a criterion described by Pistoia et al. [19] was determined for the axial compression test.

In addition to the comparison between XLH patients and their matched normal controls, we also compared the HRpQCT results with a Canadian normal population [20] by using a web portal (Normative©, v2.0, https://www.normative.ca).

2.4. Statistical analyses

Each XLH patient was pair-matched with several healthy controls based on age, sex, and BMI. Comparison of each continuous variable between XLH patients and their matched controls was conducted using a

paired *t*-test with multiple controls, as outlined by Ury et al. [21]. In HRpQCT analysis, we assessed 12 parameters at both the tibia and radius. Significance was determined after Bonferroni correction for multiple testing on the 12 parameters, with a threshold of $P \leq 0.004$ considered significant.

To compare BMD evaluation between DXA and HRpQCT, bivariate correlation analyses were performed using Spearman's correlation tests for XLH patients. These calculations were executed using SPSS Statistics software version 24.0 (SPSS, Inc., Chicago, Illinois).

3. Results

The study enrolled fourteen adult patients with XLH and thirty-four matched healthy controls (see Table 1). Among the fourteen XLH patients, six received conventional therapy (phosphorus and calcitriol) during childhood, while another six received it during adulthood. Mean serum levels of phosphorus and TmP/GFR were low, as anticipated. Serum PTH levels were slightly elevated compared to normal values, despite serum calcium and 25OHD levels falling within the expected normal range. Further detailed characteristics of XLH patients and their matched controls are presented in Supplemental Tables 1 & 2.

3.1. Bone mineral density and microarchitecture

At the lumbar spine, areal BMD (aBMD) was significantly higher in XLH patients compared to controls (Lumbar spine: aBMD mean difference = 0.319 g/cm^2, SD = 0.08, *P* value = 0.003, Z score mean difference = +2.47 SD, SD = 0.56, *P* value = 0.001, see Fig. 1A). Trabecular Bone Score was also higher in XLH patients compared to their matched healthy controls (TBS mean difference = +0.182, SD = 0.048, *P* value = 1×10^{-4}, see Fig. 1B).

Evaluation of aBMD at the radius was available for 10 XLH patients and 33 controls. Areal BMD at the distal third radius was lower in XLH patients compared to healthy controls (aBMD Z score mean difference = −1.68 DS, SD = 0.42, *P* value = 0.01) (see Fig. 1E), whereas no significant difference was found at the ultra-distal site (see Fig. 1F).

HRpQCT was performed at the distal radius (see Table 2) and tibia (see Table 3). Compared to their controls, XLH patients had wider long bones with higher total bone area at both sites. Tt.vBMD and Tb.vBMD were lower in XLH patients at both sites. Ct.Th was only lower at the radius however Ct.Area was similar to controls at both sites. At both sites, BV/TV was lower in XLH patients, with lower Tb.N and higher Tb.Sp, but Tb.Th was unaffected. Inhomogeneity of Network was also higher in XLH patients. Similar results were found when compared to a Canadian normal population (see Supplemental Figs. 1 to 4).

Bone mechanical properties evaluated by microFE analyses demonstrated unaffected Bone Stiffness and Failure Load at both sites (see Table 2 & 3).

Table 1
Anthropometric and biological measurements in cases and controls.

	XLH (n = 14)		Controls (n = 34)	
	Mean, N	SD, %	Mean, N	SD, %
Age (years)	50	15	50	15
Female sex	9	65	22	65
Weight (kg)	64.8	18.7	71.8	15.7
Height (cm)	155.6*	13	167.9	9.5
BMI (kg/m^2)	26.6	6.6	25.3	3.8
Serum PO_4^- (mmol/l)	0.58	0.1	N [0.74–1.52]	
PTH (pg/l)	69.55	37.6	N [15–65]	
25OHD (ng/ml)	32.77	13.58	N [20–80]	
ALP (UI/L)	85	31.5	N [40–150]	
BSALP (μg/L)	29.3	14.3	*N* < 22	
TmP/GFR (mmol/l)	0.37	0.13	*N* > 0.8	

N = normal ranges.
* *P* value < 0.01.

3.2. Correlations between biochemical assays, areal and volumetric BMD

In XLH patients, Tt.vBMD, Tb.vBMD and BV/TV at the radius exhibited significant correlations with aBMD at the ultra-distal radius, as well as at the total hip and femoral neck (see Table 4). Ct.vBMD also showed correlations with serum phosphate levels and aBMD at the ultra-distal radius. At the tibia, Tt.vBMD, Tb.vBMD and BV/TV were significantly correlated with aBMD at the total hip, femoral neck, distal third radius (see Table 4). Notably, PTH demonstrated inverse correlations with total vBMD and trabecular bone parameters as measured by HRpQCT. Additionally, Ct.vBMD correlated with aBMD at the ultra-distal radius, mirroring the findings observed at the radius.

3.3. Follow-up of microarchitecture and volumetric BMD over 4 years

Nine out of fourteen patients underwent a second measurement of microarchitecture by HRpQCT after a mean interval of 4.1 ± 0.3 years. The average overlap between these scans was 91 %. At the tibia, both Tt.vBMD and Ct.vBMD exhibited a significant decrease between baseline and follow-up (see Fig. 2A and Supplemental Table 3). When comparing the changes from each XLH subject to age- and sex-matched individuals from a Canadian population using the Normative.ca web database, we observed that the majority of significant abnormal decreases in vBMD were evident in post-menopausal women. Additionally, Ct.Area decreased, while Tb.Area increased, indicative of trabecularization of cortical bone at the tibia (see Supplemental Table 3). Conversely, at the radius, no significant difference was observed in other BMD or microarchitecture parameters over time. Baseline serum phosphate or PTH were not associated with any change in HRpQCT parameters.

4. Discussion

This study confirms site-specific impairment of bone microarchitecture and density in adult XLH patients, characterized by elevated bone mineral density and preserved trabecular microarchitecture at the axial skeleton, and reduced bone mineral density with trabecularization of cortical bone at the appendicular skeleton. Bone mineral density assessment, feasible through HRpQCT at the radius and tibia, revealed a worsening trend over time, particularly notable in post-menopausal women. Despite the limited accessibility of HRpQCT, our interest in identifying significant correlations between HRpQCT findings and DXA at various sites stems from the latter's practicality for routine clinical monitoring. We also report an inverse association between PTH and total vBMD and trabecular vBMD at the tibia at baseline. However, the lack of correlation between baseline PTH levels and change in vBMD overtime, as well as the small sample size, does not allow us to assess the causal nature of the association.

Of significance, our study highlights the role of distal metaphysis enlargement in maintaining bone strength in long bones, aligning with the observation that XLH patients are generally not at high risk of peripheral fractures [22]. Pseudofractures of the long bones may occur, but in general in regions with increased mechanical stress due to limb deformities [1]. MicroFE analyses revealed normal compression stiffness and maximum failure load at both sites, consistent with previous findings [23]. However, the observed enlargement of bone metaphysis during growth suggests an adaptation of the appendicular skeleton to volumetric BMD defects.

These divergent results could be due to the small sample size of each study with heterogeneous populations (receiving conventional therapy or not) or due to the selection method of controls, who were mainly matched for age and sex (except in Ni et al. study). While our findings underscore the potential utility of DXA for monitoring bone mineral density defects, especially at the distal radius, several limitations warrant consideration.

Our reliance on a fixed offset for the region of interest of HRpQCT scans may affect the paired statistics because, of these pairs, XLH

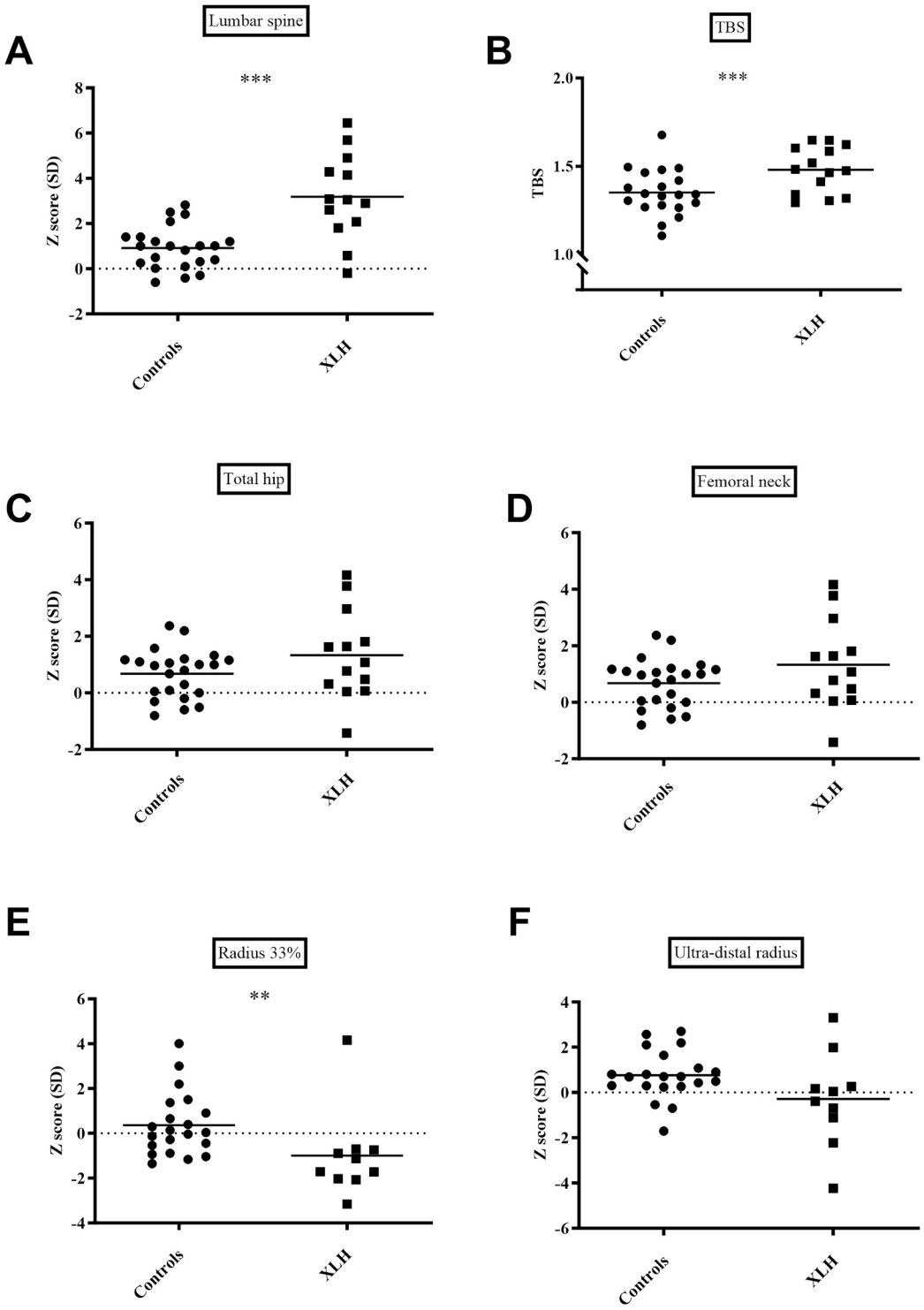

Fig. 1. Baseline BMD by DXA and Trabecular Bone Score.
A, C, D, E, F. Bone mineral density at different sites measured by DXA in controls and patients with XLH expressed in Z scores (Radius 33 % corresponds to the distal third of radial diaphysis.). B. Trabecular Bone Score (TBS) at the lumbar spine in controls and patients with XLH. ***: *P* value < 0.001; **: *P* value < 0.01 from paired *t*-test with multiple controls.

patients generally have shorter limbs. It won't, however, affect the statistics of the follow-up study where each patients is its own control.

Furthermore, our study's exploratory nature precluded analysis of therapy effects, despite evidence suggesting potential improvements in cortical parameters with specific treatments. Previous studies in children and adult XLH patients analyzed bone microarchitecture and volumetric bone mineral density by pQCT or HRpQCT according to current or past therapy status [23,24]. The authors conclude that treatment with active vitamin D and phosphorus supplementation during childhood could improve cortical thickness or mineralization.

High aBMD at the lumbar spine is a well characterized feature of XLH, even in young patients, consistent in many published studies [25–27]. In adults, the apparent high values for aBMD may be confounded by enthesophytes, but histologic analyses of iliac crest bone

Table 2
Volumetric BMD, bone microarchitecture and micro-Finite Element results evaluated from HRpQCT scans at the radius.

	Group statistics (mean ± SD)		Paired statistics			
	XLH n = 14	Controls n = 34	Mean difference	Relative difference (%)	SD*	*P* value for multiple controls#
Volumetric BMD						
Tt,vBMD (mg HA/cm^3)	251.9 ± 71.6	332.7 ± 63.8	−87.85	−26.4	22.24	0.001
Ct,vBMD (mg HA/cm^3)	966.4 ± 38.1	984.4 ± 58.7	−24.49	−2.5	14.62	0.11
Tb,vBMD (mg HA/cm^3)	126.5 ± 65.4	164 ± 33.1	−39.89	−24.3	18.45	0.05
Bone microarchitecture						
Total,Area (mm^2)	361.4 ± 79	280.3 ± 80.8	82.56	29.4	25.53	0.006
Ct,Area (mm^2)	59 ± 13.5	60.4 ± 12.1	−2.13	−3.5	4.21	0.62
Tb,Area (mm^2)	285.4 ± 45.8	224.9 ± 62.1	85.07	37.8	23.11	0.002
Ct,Th (μm)	796.9 ± 136.9	949.8 ± 178.2	−165.27	−17.4	48.42	0.004
BV/TV (%)	0.106 ± 0.054	0.137 ± 0.028	−0.033	−24.1	0.015	0.05
Tb,N (1/mm^2)	1.4 ± 0.3	2 ± 0.2	−0.6	−30.0	0.1	<0.001
Tb,Th (μm)	73.3 ± 29.7	67.8 ± 11.2	4.77	7.0	8.17	0.59
Tb,Sp (μm)	680.4 ± 231.7	436.8 ± 63.7	246	56.3	62.95	0.002
Inhomogeneity of network (μm)	385.6 ± 247.4	183.5 ± 38.1	204	111.2	66.47	0.008
Micro-finite element analysis						
Failure load (kN)	4.2 ± 1.8	4.1 ± 1.1	−0.23	−5.6	510.62	0.92
Scomp (kN/mm)	82.9 ± 36.2	81.3 ± 21.6	0.80	1.0	10.42	0.99
Sbend.Trans (kN mm/rad)	4880.7 ± 2932.0	3676.5 ± 1578.9	1148.5	31.2	832	0.19
Sbend.Sag (kN mm/rad)	3515.1 ± 1985.7	2819.4 ± 1638.5	605.8	21.5	605.44	0.33
Stors (kN mm/rad)	2729.1 ± 1534.5	1991.1 ± 977.2	695.22	34.9	445.42	0.14

* SD refers to the mean difference.
\# *P* value for multiple controls refers to mean difference.

Table 3
Volumetric BMD, Bone microarchitecture and micro-Finite Element results evaluated from HRpQCT scans at the tibia.

	Group statistics (mean ± SD)		Paired statistics			
	XLH n = 14	Controls n = 34	Mean difference	Relative difference (%)	SD*	*P* value for multiple controls#
Volumetric BMD						
Tt.vBMD (mg HA/cm^3)	250.5 ± 83	300.8 ± 44.7	−50.85	−16.9	23.560	0.05
Ct.vBMD (mg HA/cm^3)	905.2 ± 87.3	930.2 ± 69.6	−34.20	−3.7	26.405	0.21
Tb.vBMD (mg HA/cm^3)	132.6 ± 63.5	172.7 ± 40	−39.09	−22.6	18.395	0.05
Bone microarchitecture						
Total.Area (mm^2)	833 ± 193	740 ± 176	93.32	12.6	60.20	0.14
Ct.Area (mm^2)	126.3 ± 51.4	126.1 ± 25	−0.32	−0.3	14.44	0.98
Tb.Area (mm^2)	716 ± 111	621 ± 134	95.13	15.3	54.77	0.10
Ct.Th (μm)	1222.8 ± 477.5	1268.4 ± 200.7	−0.06	0.0	0.13	0.68
BV/TV (%)	0.111 ± 0.053	0.144 ± 0.033	−0.03	−20.8	0.02	0.05
Tb.N (1/mm^2)	1.64 ± 0.48	2.03 ± 0.37	−0.39	−19.2	0.15	0.02
Tb.Th (μm)	65.6 ± 21.3	71.1 ± 12.4	−4.90	−6.9	6.09	0.43
Tb.Sp (μm)	598.9 ± 221.1	438.8 ± 97.9	162.00	36.9	61.61	0.02
Inhomogeneity of network (μm)	298 ± 169	188.4 ± 53.2	110.00	58.4	46.15	0.03
Micro-finite element analysis						
Failure load (kN)	10.1 ± 4.1	11.2 ± 3	1.04	9.3	1.23	0.38
Scomp (kN/mm)	200.9 ± 83.9	221.3 ± 59.9	−20.82	−9.4	24.8	0.42
Sbend.Trans (kN mm/rad)	19,645.3 ± 11,347.1	18,018.5 ± 8573.1	1521.4	8.4	3394.3	0.66
Sbend.Sag (kN mm/rad)	21,972.1 ± 13,333.2	21,643.0 ± 10,258.3	332.56	1.5	4003.37	0.94
Stors (kN mm/rad)	13,843.9 ± 8142.5	13,046.3 ± 6043.8	752.78	5.8	2427.18	0.76

* SD refers to the mean difference.
\# *P* value for multiple controls refers to mean difference.

biopsies confirmed a high bone mass with excess osteoid tissue [26]. We here found that Trabecular Bone Score was high in XLH adults, although we acknowledge this method has some limitations to evaluate microarchitecture at the spine, as compared to histomorphometry using bone biopsies. These results are in line with those of the study of Ni et al. where mean TBS was 1.475 ± 0.129 [22]. Our study protocol did not include spine QCT in our patients and controls to properly evaluate trabecular bone fraction in the axial skeleton, which is another limitation.

Notably, our study is the first to describe longitudinal changes in microarchitectural parameters and vBMD in XLH adults. While Tt.vBMD tended to decrease at the tibia due to cortical compartment trabecularization, no modifications were observed at the radius. These changes were predominantly observed in post-menopausal women, as highlighted by comparisons with Normative.ca database findings. Unfortunately, due to the small sample size, and because clinical features such as pain or pseudofractures were not systematically registered in our protocol, we could not evaluate further the clinical significance of the observed changes in HRpQCT.

The monitoring of children or adults with XLH by DXA is not part of the different international recommendations for the management of this rare disease [5–7,28]. However, the assessment of DXA at the distal radius was missing in the studies on which these recommendations were based. Also, using pQCT, Cheung et al. observed that vBMD was elevated in children treated with conventional therapy but low in older adults who discontinued therapy or were never treated. Finally, in nutritional rickets, therapeutic interventions show evidence of improvement of DXA at the distal forearm [29]. Altogether, BMD, in particular at the

Table 4
Correlations between biological parameters and aBMD at the 3 sites with HRpQCT parameters.

		HRpQCT									
		Tibia					Radius				
		Total vBMD	Cortical vBMD	Trabecular vBMD	BV/TV	Failure load	Total vBMD	Cortical vBMD	Trabecular vBMD	BV/TV	Failure load
Serum phosphate	*Spearman rho*	−0.227	0.498	−0.276	−0.273	0.340	−0.190	**0.615***	−0.428	−0.428	0.099
	P value	0.435	0.070	0.340	0.346	0.235	0.516	**0.019**	0.127	0.127	0.736
PTH	*Spearman rho*	**−0.758****	−0.064	**−0.802****	**−0.818****	**0.618**	−0.516	−0.200	−0.385	−0.385	0.420
	P value	**0.002**	0.829	**0.001**	**0.000**	**0.019**	0.059	0.493	0.175	0.175	0.135
LS aBMD	*Spearman rho*	0.434	0.264	0.489	0.514	−0.473	0.423	0.247	0.434	0.434	−0.511
	P value	0.138	0.384	0.090	0.072	0.103	0.150	0.415	0.138	0.138	0.074
TH aBMD	*Spearman rho*	**0.725****	0.170	**0.758****	**0.754****	**-0.808****	**0.764****	−0.027	**0.802****	**0.802****	**-0.786****
	P value	**0.005**	0.578	**0.003**	**0.003**	**0.001**	**0.002**	0.929	**0.001**	**0.001**	**0.001**
FN aBMD	*Spearman rho*	**0.659***	0.330	**0.802****	**0.795****	**-0.720**	**0.720****	0.093	**0.758****	**0.758****	**-0.703**
	P value	**0.014**	0.271	**0.001**	**0.001**	**0.006**	**0.006**	0.762	**0.003**	**0.003**	**0.007**
Radius 33% aBMD	*Spearman rho*	**0.758***	0.321	**0.648***	**0.657***	**-0.879****	0.503	0.309	0.418	0.418	**-0.818****
	P value	**0.011**	0.365	**0.043**	**0.039**	**0.001**	0.138	0.385	0.229	0.229	**0.004**
Radius UD aBMD	*Spearman rho*	0.624	**0.673***	0.539	0.547	−0.624	**0.733***	0.588	**0.673***	**0.673***	**-0.818****
	P value	0.054	**0.033**	0.108	0.102	0.054	**0.016**	0.074	**0.033**	**0.033**	**0.004**

LS: Lumbar spine; TH: total hip; FN: femoral neck; UD: ultra distal; aBMD: areal bone mineral density; vBMD: volumetric bone mineral density; BV/TV: bone volume/tissue volume.
* Correlation is significant at the 0.05 level (2-tailed).
** Correlation is significant at the 0.01 level (2-tailed).

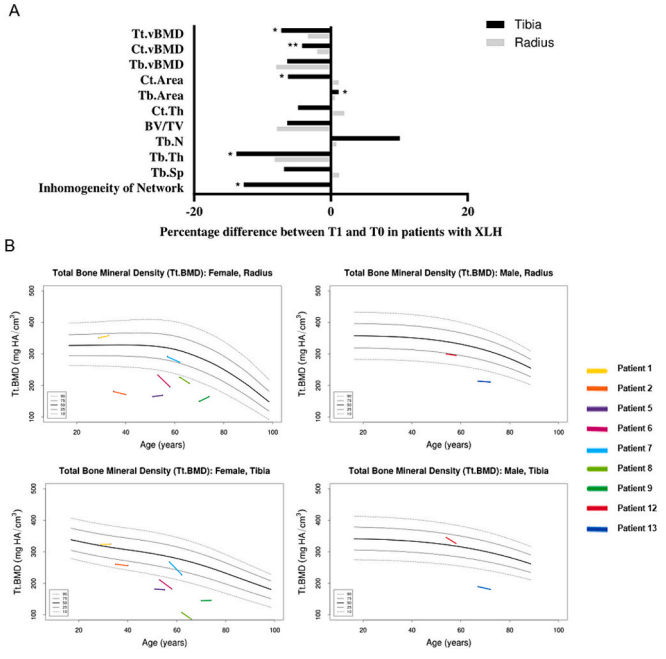

Fig. 2. Longitudinal changes in HRpQCT parameters in patients with XLH.
A. Histograms represent the mean percentage difference for each HRpQCT parameter between T1 (median of 4.1 years) and T0 (baseline) in nine adult patients with XLH. ***P* value ≤ 0.004, **P* value ≤ 0.05.
B. Colored lines represent, for each patient reported in Supplement table 2, the variation of total volumetric bone mineral density at each site (radius on the top, femur on the bottom). Age- and sex-matched percentiles were calculated from raw first-generation HRpQCT parameters (Normative©, v2.0, https://www.normative.ca) [20].

distal radius, could be a potential marker of the mineralization status of adult patients with rickets in addition to the biological hallmarks of the disease.

In conclusion, our study underscores the importance of monitoring bone mineral density in XLH patients, especially at the distal radius, which shows promise as a potential marker of mineralization status. Further investigations are warranted to evaluate the sensitivity of non-invasive methods for assessing BMD in XLH patients undergoing targeted therapies and to assess their association with clinical outcomes, particularly in comparison to serum phosphate levels. These efforts are essential for optimizing therapeutic interventions and improving the management of XLH patients in clinical practice.

CRediT authorship contribution statement

Thomas Funck-Brentano: Writing – original draft, Methodology, Formal analysis, Conceptualization. **Arnaud Vanjak:** Writing – review & editing. **Agnes Ostertag:** Formal analysis. **Maria Nethander:** Formal analysis. **Sylvie Fernandez:** Data curation. **Corinne Collet:** Conceptualization. **Didier Hans:** Software. **Bert van Rietbergen:** Writing – review & editing, Validation, Resources. **Martine Cohen-Solal:** Validation, Supervision, Methodology, Conceptualization.

Declaration of competing interest

TFB and MCS disclose their participation in a sponsored symposium by Kyowa Kirin. MCS received a research grant by Kyowa Kirin.

Data availability

Data will be made available on request.

Acknowledgments

We want to thank all patients and controls who accepted to participate in this study. We are thankful to Mrs. Sylvie Fernandez who

performed all HRpQCT acquisitions.

During the preparation of this work the authors used ChatGPT/OpenAI in order to improve the language and readability of the manuscript. After using this tool, the authors reviewed and edited the content as needed and take full responsibility for the content of the publication.

Appendix A. Supplementary data

Supplementary data to this article can be found online at https://doi.org/10.1016/j.bone.2024.117179.

References

[1] T.O. Carpenter, E.A. Imel, I.A. Holm, S.M. Jan de Beur, K.L. Insogna, A clinician's guide to X-linked hypophosphatemia, J. Bone Miner. Res. 26 (2011) 1381–1388, https://doi.org/10.1002/jbmr.340.

[2] T.O. Carpenter, E.A. Imel, M.D. Ruppe, T.J. Weber, M.A. Klausner, M.M. Wooddell, T. Kawakami, T. Ito, X. Zhang, J. Humphrey, K.L. Insogna, M. Peacock, Randomized trial of the anti-FGF23 antibody KRN23 in X-linked hypophosphatemia, J. Clin. Investig. 124 (2014) 1587–1597, https://doi.org/10.1172/JCI72829.

[3] T.O. Carpenter, M.P. Whyte, E.A. Imel, A.M. Boot, W. Högler, A. Linglart, R. Padidela, W. van't Hoff, M. Mao, C.-Y. Chen, A. Skrinar, E. Kakkis, J. San Martin, A.A. Portale, Burosumab therapy in children with X-linked hypophosphatemia, N. Engl. J. Med. 378 (2018) 1987–1998, https://doi.org/10.1056/NEJMoa1714641.

[4] K.L. Insogna, K. Briot, E.A. Imel, P. Kamenický, M.D. Ruppe, A.A. Portale, T. Weber, P. Pitukcheewanont, H.I. Cheong, S.J. de Beur, Y. Imanishi, N. Ito, R. H. Lachmann, H. Tanaka, F. Perwad, L. Zhang, C.-Y. Chen, C. Theodore-Oklota, M. Mealiffe, J.S. Martin, T.O. Carpenter, A randomized, double-blind, placebo-controlled, phase 3 trial evaluating the efficacy of burosumab, an anti-FGF23 antibody, in adults with X-linked hypophosphatemia: week 24 primary analysis, J. Bone Miner. Res. 33 (2018) 1383–1393, https://doi.org/10.1002/jbmr.3475.

[5] C.F. Munns, H.-W. Yoo, M.Y. Jalaludin, R. Vasanwala, M. Chandran, Y. Rhee, W. M. But, A.P.-S. Kong, P.-H. Su, N. Numbenjapon, N. Namba, Y. Imanishi, R. J. Clifton-Bligh, X. Luo, W. Xia, Asia-Pacific consensus recommendations on X-linked hypophosphatemia: diagnosis, multidisciplinary management, and transition from pediatric to adult care, JBMR Plus 7 (2023) e10744, https://doi.org/10.1002/jbm4.10744.

[6] D. Haffner, F. Emma, D.M. Eastwood, M.B. Duplan, J. Bacchetta, D. Schnabel, P. Wicart, D. Bockenhauer, F. Santos, E. Levtchenko, P. Harvengt, M. Kirchhoff, F. Di Rocco, C. Chaussain, M.L. Brandi, L. Savendahl, K. Briot, P. Kamenicky, L. Rejnmark, A. Linglart, Clinical practice recommendations for the diagnosis and management of X-linked hypophosphataemia, Nat. Rev. Nephrol. 15 (2019) 435–455, https://doi.org/10.1038/s41581-019-0152-5.

[7] M.R. Laurent, J. De Schepper, D. Trouet, N. Godefroid, E. Boros, C. Heinrichs, B. Bravenboer, B. Velkeniers, J. Lammens, P. Harvengt, E. Cavalier, J.-F. Kaux, J. Lombet, K. De Waele, C. Verroken, K. van Hoeck, G.R. Mortier, E. Levtchenko, J. Vande Walle, Consensus recommendations for the diagnosis and management of X-linked hypophosphatemia in Belgium, Front. Endocrinol. (Lausanne) 12 (2021) 641543, https://doi.org/10.3389/fendo.2021.641543.

[8] D. González-Lamuño, A. Lorente Rodríguez, M.I. Luis Yanes, S. Marín-del Barrio, G. Martínez Díaz-Guerra, P. Peris, Clinical practice recommendations for the diagnosis and treatment of X-linked hypophosphatemia: a consensus based on the ADAPTE method, Med. Clin. (Barc.) 159 (152) (2022) e1–152.e12, https://doi.org/10.1016/j.medcle.2021.07.026.

[9] A. Ostertag, G.E. Papadakis, C. Collet, S. Trabado, L. Maione, N. Pitteloud, J. Bouligand, M.C. De Vernejoul, M. Cohen-Solal, J. Young, Compromised volumetric bone density and microarchitecture in men with congenital hypogonadotropic hypogonadism, J. Clin. Endocrinol. Metabol. 106 (2021) e3312–e3326, https://doi.org/10.1210/clinem/dgab169.

[10] A. Bertholet-Thomas, D. Claramunt-Taberner, S. Gaillard, G. Deschênes, E. Sornay-Rendu, P. Szulc, M. Cohen-Solal, S. Pelletier, M.-C. Carlier, P. Cochat, J. Bacchetta, Teenagers and young adults with nephropathic cystinosis display significant bone disease and cortical impairment, Pediatr. Nephrol. 33 (2018) 1165–1172, https://doi.org/10.1007/s00467-018-3902-x.

[11] A. Ostertag, C. Collet, C. Chappard, S. Fernandez, E. Vicaut, M. Cohen-Solal, M.-C. de Vernejoul, A case-control study of fractures in men with idiopathic osteoporosis: fractures are associated with older age and low cortical bone density, Bone 52 (2013) 48–55, https://doi.org/10.1016/j.bone.2012.09.020.

[12] S. Fabre, M. Bourmaud, G. Mabilleau, R. Goulet, A. Couturier, A. Dentel, S. Picaud, T. Funck-Brentano, C. Collet, M. Cohen-Solal, Lrp5 p.Val667Met variant compromises bone mineral density and matrix properties in osteoporosis, JBMR Plus 7 (2023) e10741, https://doi.org/10.1002/jbm4.10741.

[13] D. Hans, A.L. Goertzen, M.-A. Krieg, W.D. Leslie, Bone microarchitecture assessed by TBS predicts osteoporotic fractures independent of bone density: the Manitoba study, J. Bone Miner. Res. 26 (2011) 2762–2769, https://doi.org/10.1002/jbmr.499.

[14] S. Boutroy, D. Hans, E. Sornay-Rendu, N. Vilayphiou, R. Winzenrieth, R. Chapurlat, Trabecular bone score improves fracture risk prediction in non-osteoporotic women: the OFELY study, Osteoporos. Int. 24 (2013) 77–85, https://doi.org/10.1007/s00198-012-2188-2.

[15] A. Ostertag, M. Cohen-Solal, M. Audran, E. Legrand, C. Marty, D. Chappard, M.-C. de Vernejoul, Trabecular and cortical bone microarchitecture alterations contribute independently to vertebral fractures in men with idiopathic osteoporosis, Osteoporos. Int. 20 (2009) 9–10.

[16] E.A.C. de Waard, C. Sarodnik, A. Pennings, J.J.A. de Jong, H.H.C.M. Savelberg, T. A. van Geel, C.J. van der Kallen, C.D.A. Stehouwer, M.T. Schram, N. Schaper, P. C. Dagnelie, P.P.M.M. Geusens, A. Koster, B. van Rietbergen, J.P.W. van den Bergh, Reliability of HR-pQCT derived cortical bone structural parameters when using uncorrected instead of corrected automatically generated endocortical contours in a cross-sectional study: the Maastricht study, Calcif. Tissue Int. 103 (2018) 252–265, https://doi.org/10.1007/s00223-018-0416-2.

[17] D.E. Whittier, S.K. Boyd, A.J. Burghardt, J. Paccou, A. Ghasem-Zadeh, R. Chapurlat, K. Engelke, M.L. Bouxsein, Guidelines for the assessment of bone density and microarchitecture in vivo using high-resolution peripheral quantitative computed tomography, Osteoporos. Int. 31 (2020) 1607–1627, https://doi.org/10.1007/s00198-020-05438-5.

[18] J.J.A. de Jong, P.C. Willems, J.J. Arts, S.G.P. Bours, P.R.G. Brink, T.A.C.M. van Geel, M. Poeze, P.P. Geusens, B. van Rietbergen, J.P.W. van den Bergh, Assessment of the healing process in distal radius fractures by high resolution peripheral quantitative computed tomography, Bone 64 (2014) 65–74, https://doi.org/10.1016/j.bone.2014.03.043.

[19] W. Pistoia, B. van Rietbergen, E.-M. Lochmüller, C.A. Lill, F. Eckstein, P. Rüegsegger, Estimation of distal radius failure load with micro-finite element analysis models based on three-dimensional peripheral quantitative computed tomography images, Bone 30 (2002) 842–848, https://doi.org/10.1016/s8756-3282(02)00736-6.

[20] L.A. Burt, Z. Liang, T.T. Sajobi, D.A. Hanley, S.K. Boyd, Sex- and site-specific normative data curves for HR-pQCT, J. Bone Miner. Res. 31 (2016) 2041–2047, https://doi.org/10.1002/jbmr.2873.

[21] H.K. Ury, Efficiency of case-control studies with multiple controls per case: continuous or dichotomous data, Biometrics 31 (1975) 643–649, https://doi.org/10.2307/2529548.

[22] G. Ariceta, S.S. Beck-Nielsen, A.M. Boot, M.L. Brandi, K. Briot, C. de Lucas Collantes, F. Emma, S. Giannini, D. Haffner, R. Keen, E. Levtchenko, O. Mäkitie, M. Z. Mughal, O. Nilsson, D. Schnabel, L. Tripto-Shkolnik, J. Liu, A. Williams, S. Wood, M.C. Zillikens, The International X-Linked Hypophosphatemia (XLH) registry: first interim analysis of baseline demographic, genetic and clinical data, Orphanet J. Rare Dis. 18 (2023) 1–17, https://doi.org/10.1186/s13023-023-02882-4.

[23] V.V. Shanbhogue, S. Hansen, L. Folkestad, K. Brixen, S.S. Beck-Nielsen, Bone geometry, volumetric density, microarchitecture, and estimated bone strength assessed by HR-pQCT in adult patients with hypophosphatemic rickets, J. Bone Miner. Res. 30 (2015) 176–183, https://doi.org/10.1002/jbmr.2310.

[24] M. Cheung, P. Roschger, K. Klaushofer, L.-N. Veilleux, P. Roughley, F.H. Glorieux, F. Rauch, Cortical and trabecular bone density in X-linked hypophosphatemic rickets, J. Clin. Endocrinol. Metabol. 98 (2013) E954–E961, https://doi.org/10.1210/jc.2012-4133.

[25] M.B. Oliveri, H. Cassinelli, C. Bergadá, C.A. Mautalen, Bone mineral density of the spine and radius shaft in children with X-linked hypophosphatemic rickets (XLH), Bone Miner. 12 (1991) 91–100.

[26] I.R. Reid, W.A. Murphy, D.C. Hardy, S.L. Teitelbaum, M.A. Bergfeld, M.P. Whyte, X-linked hypophosphatemia: skeletal mass in adults assessed by histomorphometry, computed tomography, and absorptiometry, Am. J. Med. 90 (1991) 63–69, https://doi.org/10.1016/0002-9343(91)90507-T.

[27] S.S. Beck-Nielsen, K. Brusgaard, L.M. Rasmussen, K. Brixen, B. Brock-Jacobsen, M. R. Poulsen, P. Vestergaard, S.H. Ralston, O.M.E. Albagha, S. Poulsen, D. Haubek, H. Gjørup, H. Hintze, M.G. Andersen, L. Heickendorff, J. Hjelmborg, J. Gram, Phenotype presentation of hypophosphatemic rickets in adults, Calcif. Tissue Int. 87 (2010) 108–119, https://doi.org/10.1007/s00223-010-9373-0.

[28] L. Seefried, A. Alzahrani, P. Arango Sancho, J. Bacchetta, R. Crowley, F. Emma, J. Gibbins, A. Grandone, M.K. Javaid, G. Mindler, A. Raimann, A. Rothenbuhler, I. Tucker, L. Zeitlin, A. Linglart, X.L.H. Matters, Insights and recommendations to improve outcomes for people living with X-linked hypophosphataemia (XLH), Orphanet J. Rare Dis. 18 (2023) (2022) 333, https://doi.org/10.1186/s13023-023-02883-3.

[29] T.D. Thacher, L. Smith, P.R. Fischer, C.O. Isichei, S.S. Cha, J.M. Pettifor, Optimal dose of calcium for treatment of nutritional rickets: a randomized controlled trial, J. Bone Miner. Res. 31 (2016) 2024–2031, https://doi.org/10.1002/jbmr.2886.